Limnol. Oceanogr., 39(7), 1994, 1551–1565

Modeling phytoplankton patchiness under the influence of wind-driven currents in lakes

Jan H.G. Verhagen
Department of Water Resources and Department of Theoretical Production Ecology, Agricultural University, Wageningen, Nieuwe Kanaal 11, 6709 PA Wageningen, The Netherlands

Abstract

A model has been developed that describes phytoplankton patchiness under the influence of wind-induced circulation in lakes. It is shown that especially in large lakes the adjustment of the horizontal phytoplankton distribution to a change in windspeed (in the lower windspeed region) can take several weeks, but the vertical patchiness response is much faster, usually within 1 d. In the model presented here, the phytoplankton cells are allowed to disperse in the horizontal direction by introducing a dispersion coefficient in the wind direction that takes into account some of the effects of mixing by large-scale currents in the horizontal plane. The model shows that horizontal and vertical patchiness increases with the flotation velocity of the phytoplankton, decreases with windspeed, and decreases with the strength of the horizontal wind-induced circulation currents compared to the circulation strength in the vertical plane. Model results are in agreement with observations reported in the literature.

With the help of the model results, simulations of surface chlorophyll patterns in lakes can give important information about the general pattern of horizontal wind-driven circulation.

In lakes, wind-induced currents can cause considerable heterogeneity in the horizontal concentration distribution of phytoplankton cells, as has been reported by several investigators (e.g. Reynolds 1971). A quantitative evaluation of wind effects on surface chlorophyll *a* distribution has been made by Small (1963). If the ascending velocity of buoyant planktonic organisms is greater than the descending water velocity in the region of downwelling water near the downwind shore, then these organisms will be trapped and accumulate in the upper water layer near the downwind shore. A wind-induced circulation pattern in the vertical plane is essential for this mechanism.

Webster (1990) quantified wind effects by developing and applying a steady state advection-diffusion model for plankton dispersion in lakes in which a circulation pattern exists only in the vertical plane. Here, I present an extended version of his model. In my model, phytoplankton cells are allowed to disperse in the horizontal direction by the introduction of a dispersion coefficient in the wind direction which takes into account some of the effects of mixing by large-scale currents in the horizontal plane. The model results are compared with the observations made by George and Edwards (1976) on the effects of wind on plankton patchiness in a small Welsh lake.

Water movements in a lake under the influence of wind are complex and far from fully understood (Smith 1992). Imberger and Patterson (1991) reviewed the principal experimental and theoretical work that has been carried out on mixing and water motions in shallow and deep lakes. In a stratified lake, circulation currents are confined mainly to the epilimnion, and in a shallow lake those currents extend mainly to the bottom.

According to George (1981), lake circulation patterns can be divided into two types: the first type in its simplest form is two-dimensional in the vertical plane. The drift current in the upper water layers in the direction of the wind is exactly balanced by a return current in the deeper water layers. This form of circulation can be pictured as a "conveyor belt" running along the wind axis.

The second type of circulation occurs in a shallow lake of uniform depth (Livingstone 1954). The midlake current in the wind direction is balanced by longshore-gradient return currents. This form of circulation is restricted to the horizontal plane and no deep return currents appear (Fig. 1).

Acknowledgments

I express my gratitude to D. G. George for providing additional information to earlier observations and also to my colleagues, R. W. R. Koopmans and J. Goudriaan, and to an anonymous referee for reading the manuscript and for comments.

Notation

o	Index upper layer
b	Index bottom layer
B	Width of lake perpendicular to wind direction, m
c	Concentration of blue-green cells, No. cells m^{-3} or mg Chl a m^{-3}
D_x	Horizontal dispersion coefficient, m^2 s^{-1}
D_z	Vertical turbulent exchange coefficient between surface and bottom layer, m^2 s^{-1}
F	Flotation velocity of blue-green cells, m s^{-1}
H	Water depth of isothermal lake or depth of epilimnion in stratified lake, m
k_d	Decay coefficient of wind drift velocity with depth, m^{-1}
L	Length of lake in wind direction, m
n	Number of sampling units
s	Standard deviation
T	Time scale, s
t	Time, s
u,v	Velocity in x-direction and z-direction, m s^{-1}
u^*	Friction velocity, m s^{-1}
u_s	Drift velocity at water surface, m s^{-1}
W	Windspeed, m s^{-1}
x,z	Coordinates in wind direction and in vertical direction pointing upward, m
$\frac{X_H^*}{\bar{X}}, \frac{X_V^*}{\bar{X}}$	Measures of horizontal and vertical patchiness
α	Ratio of upper-layer thickness to water depth H
ΔL	Length of the up- and downwelling regions, m
ρ	Density of water, kg m^{-3}
τ	Shear stress at the water surface, N m^{-2}

In an irregularly shaped lake, circulation patterns become more complex and contain elements of both circulation types. The wind-induced water movements in Eglwys Nynydd, a shallow reservoir in South Wales, have been studied extensively by George and Edwards (1976) by means of free-running depth-specific drogues. Although Eglwys Nynydd is shallow (mean depth, 3.5 m) and depth does not vary greatly over the lake area, George and Edwards observed circulation to be predominantly of the conveyor-belt type. This outcome emphasizes that uncertainties still exist about how lake morphology influences circulation pattern.

Methods

In the model I propose here, the two types of wind-induced circulation are schematized as follows. In the vertical plane, the currents are described in a two-layer system. In the upper layer, of thickness αH, the drift current is in the wind direction; in the lower layer, of thickness $(1-\alpha)H$, the drift current is in the direction opposite of the wind. The factor α ranges from 0 to 1, and H is the mean water depth of the lake (Fig. 1). (A list of notation is provided.)

The horizontal coordinate in the wind direction is denoted x and the vertical coordinate pointing upward from the water surface is denoted z. The above elementary description leads to a one-dimensional, two-layer model with coordinate x and time t. The effect of the circulation pattern in the horizontal plane is reduced in this one-dimensional, two-layer model to a horizontal exchange of water masses described by a horizontal dispersion coefficient, D_x, which is assumed to be proportional to the drift velocity of the water in the layer in question.

Apart from the inclusion of horizontal mixing, my model contains the following additions to the model of Webster (1990): a more detailed description of the decrease in the vertical diffusion coefficient for windspeeds <4–5 m s^{-1}, a separate mathematical description of the up- and downwelling regions near the up- and downwind shores, and a non-steady state description.

The model equations—The variables in each layer are values averaged over the layer thickness and over the width of the lake perpendicular to the wind direction. Variables in the upper layer have the index o; those in the lower layer have the index b.

The concentration $c(x,t)$ of buoyant blue-green cells in the surface and bottom layer is described by the advection-diffusion equation.

$$\frac{\partial c_o}{\partial t} = -u_o\frac{\partial c_o}{\partial x} + D_{xo}\frac{\partial^2 c_o}{\partial x^2} - D_z\frac{(B_o + B_b)/2}{\alpha H B_o}\frac{c_o - c_b}{H/2} + F\frac{(B_o + B_b)/2}{\alpha H B_o}c_b; \quad (1)$$

$$\frac{\partial c_b}{\partial t} = u_b\frac{\partial c_b}{\partial x} + D_{xb}\frac{\partial^2 c_b}{\partial x^2} + D_z\frac{(B_o + B_b)/2}{(1-\alpha)H B_b}\frac{c_o - c_b}{H/2}$$

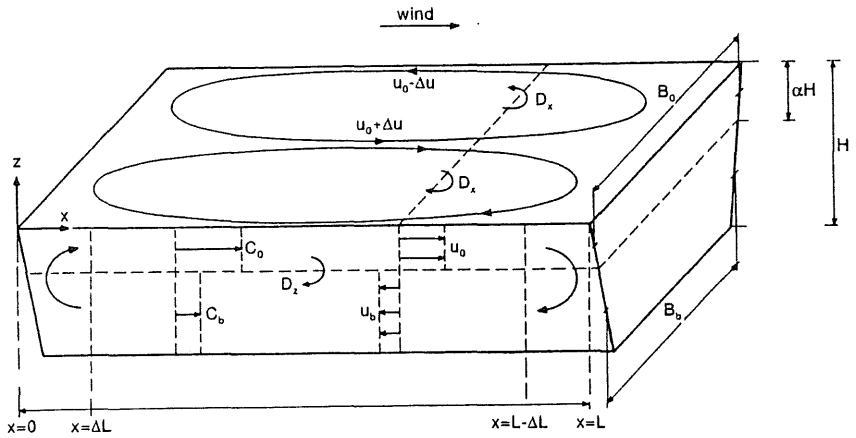

Fig. 1. Schematic representation of wind-driven circulation patterns and vertical plankton concentration distributions in an isothermal lake of depth H, or in the epilimnion of a stratified lake with thickness H.

$$- F\frac{(B_o + B_b)/2}{(1 - \alpha)HB_b}c_b. \qquad (2)$$

$c_o(x,t)$, $c_b(x,t)$: concentration of blue-green cells in the surface and bottom layer (No. m^{-3} or mg Chl a m^{-3}); $u_o(t)$, $u_b(t)$: current velocity in the surface and bottom layer (m s^{-1}).

It should be noted that the algal cells in the above diffusion-advection equation have been treated as a conservative substance (i.e. as a suspension of inert particles). In fact, the time scales for growth and decay in the number of cells have been assumed to be substantially greater than the time scales associated with a redistribution of the concentration due to the currents and the flotation velocity. Whether this assumption is justified is discussed later.

Equations 1 and 2 are valid in that region of the lake where the net vertical water velocity is negligible, i.e. in the main water domain region $\Delta L \leq x \leq L - \Delta L$, a distance ΔL away from the up- and downwind shores (L is the length of the lake in wind direction).

Each term on the right-hand side of Eq. 1 and 2 represents a contribution to the net rate of change of blue-green cell concentration in the surface and bottom layer, respectively, at a given location x and time t. The first term on the right-hand side gives the contribution due to horizontal advection, the second term the contribution due to horizontal dispersion, and the third term the contribution due to vertical turbulent exchange of cells between the surface and bottom layer. The vertical turbulent exchange transport is proportional to the boundary area $L(B_o + B_b)/2$ between both layers and inversely proportional to the exchange distance $H/2$. The last term gives the contribution due to the import of algal cells from the bottom layer or export to the surface layer.

The conservation equation for water requires that there is no net horizontal flow in the x-direction, so

$$u_o\alpha HB_o = u_b(1-\alpha)HB_b$$

or

$$u_b = \frac{\alpha B_o}{(1 - \alpha)B_b}u_o. \qquad (3)$$

Multiplying Eq. 2 by $(1 - \alpha)B_b/(\alpha B_o)$ and adding the result to Eq. 1 gives, with the use of Eq. 3,

$$\frac{\partial}{\partial t}\left[c_o + \frac{(1 - \alpha)B_b}{\alpha B_o}c_b\right] = -u_o\frac{\partial(c_o - c_b)}{\partial x} + D_{xo}\frac{\partial^2 c_o}{\partial x^2} + D_{xb}\frac{(1 - \alpha)B_b}{\alpha B_o}\frac{\partial^2 c_b}{\partial x^2}. \qquad (4)$$

Equation 4 is not independent of the first three equations. Equation 4 is introduced here only because it appears convenient later on to replace Eq. 2 with Eq. 4. The variables u_o, D_{xo}, D_{xb}, and D_z are functions of the windspeed and are specified in the next pages.

Relation between u_o *and windspeed*—Empirical observations given by Smith (1992) indicate that the relation between wind and current speed at the water surface, u_s, shows a discontinuous behavior at windspeeds of 4–5 m s^{-1}. This sudden change in the interaction between wind and water is often explained as being due to a change in downward energy transport as wave crests start to spill over at windspeeds >4–5 m s^{-1}.

The ratio of surface current speed to windspeed W (called the wind factor) was measured in Eglwys Nynydd by George and Edwards (1976). They found that the wind factor decreased with increasing windspeed and remained constant at 0.005 above a critical windspeed of ~5 m s^{-1}. The reported regression line fitted to the data is

$$\begin{aligned} u_s/W &= 0.03(1 - W/6) \quad \text{for } W \le 5 \text{ m s}^{-1}, \\ &= 0.005 \quad \text{for } W > 5 \text{ m s}^{-1}. \end{aligned} \tag{5}$$

The ratio between u_s and u_o follows from information about the velocity depth profile.

In the literature, there are several suggestions about the form of the velocity depth profile. The quadratic velocity profile given by Banks (1975) is well known:

$$u/u_s = (1 + z/H)\,(1 + 3z/H). \tag{6}$$

Observe that $u/u_s = 0$ for $z/H = -1/3$ leading to $\alpha = 1/3$ in that case.

Logarithmic velocity profiles have been proposed by several investigators (e.g. Cheung and Street 1988). A feature of all these relations is that the profile form, whether it is quadratic or logarithmic, remains the same at all windspeeds, which is not in accordance with observations. Smith (1979) therefore suggested an exponential decline in wind drift velocity with depth near the water surface:

$$u = u_s \exp(k_d\, z).$$

The decay coefficient k_d is a decreasing empirical function of windspeed:

$$k_d = 6.0\, W^{-1.84}. \tag{7}$$

George and Edwards (1976) also observed that the ratio of the current speeds measured at 0.5 and 1.0 m below the water surface changed appreciably with windspeed. At windspeeds <4 m s^{-1}, they found turbulent transport of momentum to be weak, with current speed declining rapidly with depth in the upper water layers. As the windspeed rises, vertical turbulent transfer of momentum tends to equalize currents measured at 0.5 and 1.0 m below the water surface. George and Edwards suggested that the effect of windspeed on the transport of plankton cells will be more or less linear because the increase in vertical turbulent transport with increase in windspeed tends to compensate for the rapid decline in the wind factor with windspeed. Therefore, it is assumed that u_o is proportional to W for all values of W under consideration and equal to

$$u_o = 5 \times 10^{-3}\, W. \tag{8}$$

Relation between D_z *and windspeed*—According to the above, the vertical exchange coefficient D_z will increase rapidly with W. The value of D_z is estimated as follows. The vertical exchange coefficient between the surface and the bottom layer is assumed to be proportional to the vertical component of the turbulent eddy viscosity,

$$D_z \approx \tau/(\rho\, \mathrm{d}u/\mathrm{d}z) \tag{9}$$

where τ is the shear stress and ρ the water density.

For low windspeeds ($W < 4$ m s^{-1}), turbulent transfer of momentum is weak, and it is sufficient to estimate D_z near the water surface. Using Smith's exponential wind drift velocity profile, we can write $(\mathrm{d}u/\mathrm{d}z)_{z=0} = u_s\, k_d$, and D_z becomes

$$D_z = u^{*2}/(u_s\, k_d).$$

The friction velocity $u^* = (\tau/\rho)^{1/2}$ is proportional to the windspeed and is specified (following Webster 1990) as

$$u^* = 1.2 \times 10^{-3}\, W. \tag{10}$$

So D_z can be expressed in terms of W for small values of W.

As W rises, turbulent transfer of momentum increases and water motion is spread over the total water column. In this case, the vertical component of the turbulent eddy viscosity reaches its maximum value, which is proportional to H and can be specified as $D_z = u^*H/15$ in accordance with the specification given by Webster (1990). Summarizing, D_z is specified as

Table 1. Results for $H = 3.5$ m.

	Windspeed (m s^{-1})							
$15D_z/u^*H$	0.5	1.0	1.5	2.0	2.5	3.0	3.5	4.0
According to Eq. 11	0.009	0.034	0.080	0.153	0.264	0.431	0.687	1.0
Readjusted with Eq. 12	0.069	0.082	0.107	0.153	0.264	0.431	0.687	1.0

$$15D_z/(u^*H) = \min\{1, 0.1W^{1.84}/[(1-W/6)H]\} = G(W). \quad (11)$$

Table 1 shows results for $H = 3.5$ m (the mean water depth in Eglwys Nynydd).

As a check, it is also possible to directly use the data given in the plot $u_{0.5}/u_{1.0}$ against windspeed presented by George and Edwards as mentioned earlier. With $u_{0.5}/u_{1.0} = F(W)$ and Smith's exponential velocity profile,

$$u_{0.5}/u_{1.0} = \exp(0.5k_d) = F(W). \quad (12)$$

This relation can be transformed into a plot of k_d against W, which differs from the empirical relation (Eq. 7) at low windspeeds. Therefore, the final estimate of D_z is adjusted with Eq. 12 for windspeeds <2 m s^{-1} as shown in Table 1.

Relation between D_x *and windspeed*—In a one-dimensional model, the water motion associated with the Livingstone-type circulation is transformed into a horizontal exchange of water masses described by a horizontal dispersion coefficient D_x. D_{xo} and D_{xb} are assumed to be proportional to the current speed in the surface and bottom layer.

$$D_{xo} \propto u_o L \text{ and } D_{xb} \propto u_b L.$$

L is the characteristic length of the largest horizontal eddy in the lake—in the case of Livingstone-type circulation, equal to the length of the lake in the wind direction.

Using the relations of Eq. 3 and 8 between u_o, u_b, and W, the horizontal dispersion coefficient can be written as

$$D_{xo} = \gamma WL \qquad D_{xb} = \frac{\gamma WL\alpha B_o}{(1-\alpha)B_b}. \quad (13)$$

γ is a proportionality constant.

Estimates of D_x as a function of W and L, proposed by several investigators based on observations in lakes, are summarized by Smith (1992). For windspeeds of 2–5 m s^{-1} and $L =$ 1,000 m, D_x appeared to be 2–5 m^2 s^{-1}. This indicates that γ should have an estimated magnitude of 10^{-3}.

An estimate of the characteristic length of Eglwys Nynydd, in case Livingstone-type circulation is present, has been obtained as follows. According to George and Edwards (1976), the surface area of Eglwys Nynydd is 1.01 km^2; from the given morphometric maps, the length and width of the reservoir are ~1,500 m and 675 m. The longest axis of the lake nearly coincides with the north–south direction, and the prevailing wind is from the northwest. On the basis of this information, a reasonable estimate of the length of the lake in wind direction is $L = 1{,}000$ m, which gives a horizontal dispersion coefficient of $D_x = 10^{-3}WL$. In the case where Livingstone-type circulation is not present, the largest horizontal eddy is no longer related to lake size, and the horizontal dispersion coefficient reaches a lower limit of $D_x = 2.5 \times 10^{-2}$ m^2 s^{-1}. This value appears to be the same in different lakes at different windspeeds (Smith 1992).

D_x can also be estimated directly from the experimental data presented by George and Edwards (1976). They plotted the wind factor as a function of windspeed. The variation of the data around the regression line of u_s/W against W is partly due to experimental error and partly due to variation of u_s over the lake area. The standard deviation (σ) of u_s/W was 0.2×10^{-2}.

From mixing length theory, Smith (1992) derived $D_x = \sigma WB/2$, where $B/2$ is half the width of the lake perpendicular to the wind direction and equal to the size of the largest horizontal eddy measured in that direction.

If B is assumed to equal L, $D_{xo} = 10^{-3}WL$, which implies

$$\gamma = 10^{-3}. \quad (14)$$

Flotation velocity—George and Edwards (1976) reported development of dense blooms

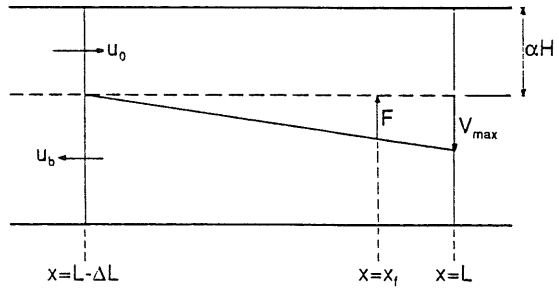

Fig. 2. Schematic representation of the downwelling current in the downwind compartment of length ΔL.

of blue-greens (principally *Microcystis aeruginosa* but also *Anabaena flos-aquae* and *Aphanizomenon* sp.) in Eglwys Nynydd in summer during their study period. Reynolds et al. (1987) estimated flotation rates ranging from 360 to -120×10^{-6} m s^{-1} for *M. aeruginosa* and 60 to -10×10^{-6} m s^{-1} and 40 to -7×10^{-6} m s^{-1} for the other two blue-greens (Webster 1990 incorrectly quoted these data from Reynolds et al., reversing sinking and flotation rates). The flotation velocity used in the model simulations is assumed to be 100 $\times 10^{-6}$ m s^{-1}, or 8.64 m d^{-1}, somewhat lower than the midrange value of the flotation velocity for *M. aeruginosa* found by Reynolds et al.

Model equations for the up- and downwind shore regions—Horizontal currents dominate in the main water body, and the contribution of vertical advective transport has been neglected in the diffusion-advection equation, as is shown in Eq. 1 and 2 for this region. In the up- and downwelling regions near the up- and downwind shores, however, the model equations should include the contribution of vertical advective transport, the derivation of which is described below. The downwind region is defined as a compartment extending from $L - \Delta L < x \leq L$. The upwind region is defined as a compartment between $0 \leq x < \Delta L$.

Kranenburg (1987) measured ΔL of the upwelling region at the upwind shore in a flume tank. He obtained $\Delta L = 7\ H$, using a windspeed of ~10 m s^{-1}. At windspeeds <5 m s^{-1}, the ratio $\Delta L/H$ will be higher due to reduction in the vertical transport of momentum at low windspeeds. The introduction of a windspeed-dependent compartment length, ΔL, complicates the numerical formulation of the problem to some extent. Such a refinement of the model description is not really necessary, so I assumed a wind-independent ratio, $\Delta L/h$. I chose the value $\Delta L/H = 20$ as an estimate of this ratio in the lower windspeed range considered here. The downwind compartment is represented in Fig. 2.

The vertical water velocity $v(x)$ through the boundary between the surface and bottom layer at $z = -\alpha\ H$ must satisfy the continuity equation in the surface layer; so

$$u_o \alpha H B_o + \frac{B_o + B_b}{2} \int_{L-\Delta L}^{L} v\, dx = 0. \quad (15)$$

Assuming $v(x)$ linear with x as shown in Fig. 2 gives us

$$v(x) = v_{max} \frac{x - (L - \Delta L)}{\Delta L}$$

where

$$v_{max} = u_o \frac{\alpha H}{\Delta L} \frac{4B_o}{B_o + B_b}. \quad (16)$$

The vertical advective transport of algal cells depends on the relative velocity between downwelling current speed and flotation velocity F. If $F > v_{max}$, then the vertical advective transport, VAT, is directed upward and is proportional to the algal concentration in the bottom layer, so

$$\text{VAT} = c_b \left(F - \frac{v_{max}}{2} \right) \frac{B_o + B_b}{2} \Delta L. \quad (17)$$

If $F < v_{max}$, then the VAT of algal cells contains two contributions, one proportional to the surface concentration and the other proportional to the bottom-layer concentration, depending on the sign of the net vertical velocity of the cells relative to downward current speed. The formulation is

$$\text{VAT} = \left[c_b F \frac{x_f - L + \Delta L}{2} - c_o (v_{max} - F) \frac{L - x_f}{2} \right] \times \frac{B_o + B_b}{2}. \quad (18)$$

x_f is the location x where the downwelling current speed just compensates the bouyancy velocity, so

$$x_f = L - \Delta L + \frac{F}{v_{\max}}\Delta L. \tag{19}$$

Substitution of Eq. 19 in 18 leads to

$$\mathrm{VAT} = \left[c_o\left(F - \frac{v_{\max}}{2}\right) - (c_o - c_b)\frac{F^2}{2v_{\max}}\right] \times \frac{B_o + B_b}{2}\Delta L. \tag{20}$$

A similar expression for the vertical transport of algae at the upwind compartment can be derived. The result is

$$\mathrm{VAT} = c_b\left(F + \frac{v_{\max}}{2}\right)\frac{B_o + B_b}{2}\Delta L \tag{21}$$

valid for all $v_{\max} \geq 0$.

Boundary conditions—At the up- and downwind shores, the net horizontal transport of algal cells in both layers must be zero. So for $x = 0$ and $x = L$:

$$\begin{aligned} u_o c_o - D_{xo}\frac{\partial c_o}{\partial x} &= 0, \\ -u_b c_b - D_{xb}\frac{\partial c_b}{\partial x} &= 0. \end{aligned} \tag{22}$$

The variables u and c in the upwind and downwind compartment of the model will be considered only as averaged values over x so the integrated form of the diffusion-advection equation can be used. With the use of boundary conditions Eq. 22, the diffusion-advection equation in the upper layer of the downwind compartment integrated over x becomes

$$\begin{aligned} \frac{dc_o}{dt} = {} & \frac{\left[u_o c_o - D_{xo}\frac{\partial c_o}{\partial x}\right]_{x=L-\Delta L}}{\Delta L} \\ & + \left\{-D_z\frac{c_o - c_b}{H/2}\right. \\ & + c_b\left(F - \frac{v_{\max}}{2}\right)\mathrm{Hs}(F - v_{\max}) \\ & + \left[c_o\left(F - \frac{v_{\max}}{2}\right) - \frac{F^2}{2v_{\max}}(c_o - c_b)\right] \\ & \left. \times \mathrm{Hs}(v_{\max} - F)\right\}\frac{B_o + B_b}{2B_o\alpha H}. \end{aligned} \tag{23}$$

Hs(s) is the Heaviside unit function defined as

$$\mathrm{Hs}(s) = \begin{cases} 0.0 & s < 0 \\ 0.5 & s = 0 \\ 1.0 & s > 0. \end{cases}$$

With the use of the boundary condition at $x = 0$, the diffusion-advection equation in the upper layer in the upwind compartment integrated over x becomes

$$\begin{aligned} \frac{dc_o}{dt} = {} & \frac{-\left(u_o c_o - D_{xo}\frac{\partial c_o}{\partial x}\right)_{x=\Delta L}}{\Delta L} \\ & + \left[-D_z\frac{c_o - c_b}{H/2} + c_b\left(F + \frac{v_{\max}}{2}\right)\right] \\ & \times \frac{B_o + B_b}{2B_o\alpha H}. \end{aligned} \tag{24}$$

The diffusion-advection equation in the whole downwind compartment integrated over x becomes

$$\begin{aligned} & \frac{d\left[c_o + \frac{(1-\alpha)B_b}{\alpha B_o}c_b\right]}{dt} \\ & = \frac{\left[u_o(c_o - c_b) - D_{xo}\frac{\partial(c_o + c_b)}{\partial x}\right]_{x=L-\Delta L}}{\Delta L}, \end{aligned} \tag{25}$$

in the whole upwind compartment

$$= \frac{-\left[u_o(c_o - c_b) - D_{xo}\frac{\partial(c_o + c_b)}{\partial x}\right]_{x=\Delta L}}{\Delta L}. \tag{26}$$

Keeping in mind that Eq. 1 and 4 are valid in the main water domain (i.e. for $\Delta L \leq x \leq L - \Delta L$), we see that the six coupled differential equations (1, 4, 23–26) describe the algal concentration in the total water domain $0 \leq x \leq L$.

These model equations can be solved numerically using the initial condition:

$$c_o(x, 0) = c_b(x, 0) = c_i = 100 \text{ mg Chl } a \text{ m}^{-3}. \tag{27}$$

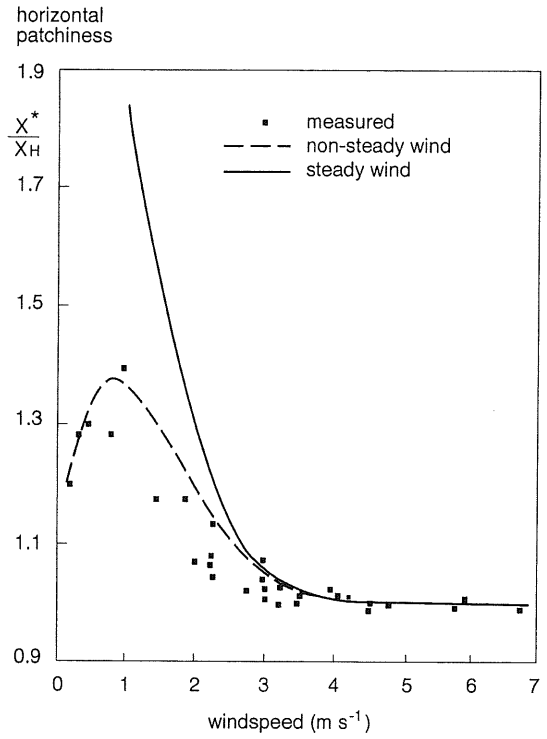

Fig. 3. The horizontal patchiness of blue-green cells as a function of windspeed in Eglwys Nynydd. Model results, based on steady and on non-steady wind conditions, are compared with observations made by George and Edwards (1976).

Results and discussion

The model results and discussion of the results center around five topics: comparison with model results from Webster (1990); comparison with observations by George and Edwards (1976) in Eglwys Nynydd; extrapolation of steady state model results to other parameter values; extrapolation of non-steady state model results to other and larger lakes; perspectives in future research opened by the model results.

Comparison with the model of Webster—My model is similar to one developed earlier by Webster (1990). An important difference from his model is inclusion of a horizontal dispersion coefficient in the wind direction.

The inclusion of a horizontal dispersion term in the model, which can take effects of Livingstone-type circulation into account, affects the model results drastically.

Webster (1990, p. 990–991) deliberately neglected the horizontal dispersion term in his advection-diffusion equation with the argument that "The coupling of turbulent diffusion in the vertical direction with a vertically sheared horizontal flow can result in very high dispersal rates in the horizontal direction through the mechanism of shear dispersion (Okubo 1971). This process is represented implicitly in the statement of Eq. 1." (Webster's equation 1 is a steady state advection-diffusion equation without a horizontal dispersion term.)

Webster's argument is not valid in this specific case. Okubo (1971) and Fischer et al. (1979) found that the dispersal rate in the horizontal direction caused by shear dispersion was proportional to the depth-averaged advective transport of the substance considered. But according to Webster's equation 5 ($\int_H^0 uc\, dz = 0$), this depth-averaged transport is zero, and the horizontal shear dispersion is therefore zero in his model.

The depth-averaged advective transport of substance is no longer zero if a horizontal dispersion term is introduced in the advection-diffusion equation. In this case, the mechanism of shear dispersion becomes active, leading to model results that can be more than one order of magnitude different from those he obtained. This outcome has been the main reason to revise the mathematical description of wind effects on the distribution of phytoplankton in lakes.

The models I present here can be reduced to Webster's model as follows. Assume, as Webster did, $\partial/\partial t = 0$, $D_{xo} = D_{xb} = 0$, $B_o = B_b$, and $D_z = u^*H/15$, Eq. 1 reduces to

$$0 = -u_o \frac{dc_o}{dx} - \frac{u^*}{15\alpha} \frac{c_o - c_b}{H/2} + \frac{F}{\alpha H} c_b, \quad (28)$$

and Eq. 4 reduces to

$$0 = -u_o \frac{d(c_o - c_b)}{dx}. \quad (29)$$

Equations 25 and 26 reduce to the boundary condition

$$0 = u_o(c_o - c_b) \quad (30)$$

for $x = \Delta L$ and $x = L - \Delta L$. Equations 28 and 29, together with the boundary condition Eq. 30, can easily be solved yielding

$$c_o = c_b = c_{x=0}\exp\left(\frac{Fx}{u_o \alpha H}\right). \quad (31)$$

This analytical result can be compared with the numerical solution found by Webster:

$$c_o \approx c_b \approx c_{x=0}\exp\left(\frac{1.33Fx}{u^* H}\right). \quad (32)$$

Webster used a quadratic vertical velocity profile, $u(z)$, specified in his equation 10, from which α can be obtained from $u(-\alpha H) = 0$ and u_o from the equation

$$u_o = \frac{1}{\alpha H}\int_{-\alpha H}^{0} u(z)\, dz. \quad (33)$$

The result is

$$\alpha = 0.4253 \text{ and } u_o = 2.3034\, u^*. \quad (34)$$

Substituting these values in the exponent of Eq. 31 gives

$$1.021\, Fx/u^* H.$$

This result is nearly identical to Webster's model. The small numerical difference in the proportionality constant contained in the exponent, 1.021 vs. 1.33, can be attributed to differences in model formulation—the present two-layer model vs. his multilayer model with a specified velocity profile.

This similarity in results is no longer present when more realistic values of D_x are introduced, as shown below. As an example, the phytoplankton concentration calculated with the present model shows in most cases a pronounced vertical gradient, contrary to the nearly uniform vertical distribution found by Webster.

Comparison with the observations of George and Edwards—Spatial dispersion of natural populations is often quantified in terms of the variance s^2 to arithmetic mean

$$\bar{X} = \frac{1}{n}\sum_{1}^{n} x^n$$

ratio in the counts $x_1, x_2, x_3, \ldots, x_n$ of sampling units of number n. There are many variants of this ratio. George and Edwards (1976) used the ratio of mean crowding X^* to mean density $\bar{X}$ as the measure of patchiness.

They defined mean crowding as

$$X^* = \bar{X} + \frac{s^2}{\bar{X}} - 1. \quad (35)$$

For the case of a large number of sampling units, the measure of patchiness can be written as

$$\frac{X^*}{\bar{X}} \approx \frac{1}{n}\frac{\sum_{1}^{n} x^2}{\bar{X}^2}. \quad (36)$$

The measure of horizontal patchiness in plankton concentration in the upper layer is therefore

$$\frac{X_H^*}{\bar{X}} = \frac{\frac{1}{L}\int_0^L c_o^2(x, t)\, dx}{\left[\frac{1}{L}\int_0^L c_o(x, t)\, dx\right]^2}, \quad (37)$$

and the measure of vertical patchiness in plankton concentration in the two-layer system becomes

$$\frac{X_v^*}{\bar{X}} = \frac{\alpha c_o^2(x, t) + (1 - \alpha)c_b^2(x, t)}{[\alpha c_o(x, t) + (1 - \alpha)c_b(x, t)]^2}. \quad (38)$$

Observe that the measure of patchiness is unity when the distribution is homogeneous.

In Fig. 3, the calculated horizontal patchiness is plotted against windspeed. The horizontal patchiness is the steady state value for an applied steady wind condition.

Comparison of my model result with the observations of George and Edwards (Fig. 3) shows some similarity in results only for windspeeds >2–3 m s^{-1}. At lower windspeeds, the calculated horizontal patchiness is much larger than measured. As the steady windspeed approaches zero, the calculated horizontal patchiness reaches a maximum value of 2.53 (*see Fig. 6*), whereas the observed horizontal patchiness reaches a maximum value of ~ 1.4 at around 1 m s^{-1}, after which it seems to decline.

The cause of the discrepancy between model results and field observations can be attributed to non-steady state effects. I explain this below in some detail and quantify the non-steady state effects with model simulations.

A number of time scales are involved in the adjustment time of the plankton distribution to a change in windspeed. For the parameter values used until now, the shortest time scale

is equal to the time it takes for a phytoplankton cell to travel the vertical distance between the centers of the upper and lower water layers. This time scale is

$$T_{min} = \min(H/2F,\ H^2/4D_z), \qquad (39)$$

corresponding to $\sim 10^4$ s or 0.1 d.

The longest time scale in the system is the mean time it takes for a phytoplankton cell to travel from one side of the lake to the other in the wind direction:

$$T_{max} = \min[2L(1-\alpha)/u_o,\ L^2/2D_x], \qquad (40)$$

which can be interpreted as the shortest circulation time belonging to either the vertical conveyor-belt circulation or the horizontal Livingstone-type circulation. So, the longest time scale is inversely proportional to the windspeed and takes a value of ~ 3 d at a windspeed of 1 m s^{-1} for the Eglwys Nynydd case.

With the above information about time scales, we can determine whether it is justified to treat algal cells as a conservative substance, as has been done here. As mentioned earlier, the assumption behind the conservative substance approach is that the time scale of growth and decay of an algal population must be large compared to the longest time scale, T_{max}. A reasonable estimate of the time scale of growth and decay of an algal population in a natural environment is ~ 10 d, so the conservative substance approach is valid in the Eglwys Nynydd case, but less justified for large lakes.

To account for non-steady state effects, George and Edwards considered only occasions when the wind direction did not change $>50°$ and applied a weighted moving-average procedure over the windspeed history for the 24 h prior to the time of sampling.

They introduced an equivalent steady windspeed, defined as

$$W_{eq}(t) = \frac{1}{\tau^*}\int_0^\infty W(t-\tau)\exp\left(-\frac{\tau}{\tau^*}\right)d\tau \qquad (41)$$

where $\tau^* = 0.24$ d.

Equation 41 is a slightly modified version of the one given by George and Edwards. The relation between their exponent 0.693 in the weighting function and τ^* used here is

$$\tau^* = (4\text{ h})/0.693 = 0.24\text{ d}.$$

The given estimate of T_{max} shows that the adjustment time of ~ 1 d assumed by George and Edwards is too short, especially at windspeeds <2 m s^{-1}.

An improved estimate of non-steady state effects on the plankton distribution could be obtained from simulations of my model based on measured data of the wind history, $W(t-\tau)$, a few days before the time of sampling, t. Because such data are not available, an assumption must be made about the most probable wind history. I have assumed that the memory in the windspeed is not >2 d, so 2 d before the time of sampling, the most probable windspeed is equal to the mean windspeed, which is 5 m s^{-1} near Eglwys Nynydd (George and Edwards 1976). In those previous 2 d, the windspeed gradually approaches the value $W(t)$ measured at the time of sampling. The assumed windspeed history is

$$\begin{aligned} W(t-\tau) &= W(t) && \text{for } 0 \le \tau \le 0.5\text{ d} \\ &= W(t) + [5 - W(t)](\tau - 0.5)/1.5 && \\ & && \text{for } 0.5 \le \tau \le 2\text{ d} \\ &= 5\text{ m s}^{-1} && \text{for } \tau \ge 2\text{ d}. \end{aligned} \qquad (42)$$

Model simulations have been carried out for various values of the windspeed at t, using the wind history over the past days according to Eq. 42. Each computation was started 5 d before t. The simulated horizontal patchiness at t has been plotted in Fig. 3 as the non-steady wind case (dashed line) for a large number of values $W(t)$. For a proper comparison with the data of George and Edwards, the simulated non-steady wind results in Fig. 3 should have been plotted against the equivalent windspeed according to Eq. 41 in which Eq. 42 has been substituted instead of $W(t)$. However, the relation between $W_{eq}(t)$ and $W(t)$ is $W_{eq}(t) = 0.98\ W(t) + 0.10$ m s^{-1}, so $W_{eq}(t)$ can be replaced by $W(t)$ without loss of accuracy.

The agreement with the observations of George and Edwards is very good, especially when we take into account the rather crude assumption about wind history. The fact that the horizontal patchiness in the observations seems to decrease as the windspeed tends to zero, producing a maximum at ~ 1 m s^{-1}, is predicted by the model simulations. It can now be explained by the time scale of adjustment

at windspeeds <1 m s^{-1}, which is longer than the memory in windspeed. Near-calm conditions do not last long enough to give the plankton distribution the opportunity to build up a substantial change in patchiness which could still be present as a result of the wind conditions more than 2 d earlier. The most probable patchiness >2 d before the time of sampling has the value 1, corresponding to a uniform plankton distribution belonging to a mean windspeed of 5 m s^{-1}.

In Fig. 4, the horizontal patchiness at steady state conditions is plotted against vertical patchiness at a representative downwind station taken at $x = 0.7L$, and comparisons are made with the observations of George and Edwards. The agreement is much better than expected, since observations are probably not all in steady state and the calculation of vertical patchiness is based on a two-layer concentration distribution in the model and in observations on only four samples in the vertical. If the results of Webster's model were plotted in Fig. 4, the result would be a nearly vertical line through the point $X^*/\bar{X}_v = 1$.

Extrapolation of steady state model results to other situations—Figures 5–7 show model results of horizontal patchiness,

$$\frac{X^*_H}{\bar{X}} = G\left(W, F, \frac{D_x}{u^*L}, \frac{L}{H}, t\right), \qquad (43)$$

for various values of the first three variables and for the steady state situation.

Figure 5 shows horizontal patchiness as a function of W for three values of F keeping $D_x/u^*L = 0.83$ and $L/H = 28.6$, the same values as in the Eglwys Nynydd case. Horizontal patchiness decreases with increasing windspeed. At zero W, $X^*_H/\bar{X}$ goes to 2.54 for all F. It must be remembered, however, that the practical value of this result is limited, because steady state at very low windspeeds is never reached.

Figure 6 shows horizontal patchiness as a function of F for three values of W. Horizontal patchiness tends to 1 as F tends to 0, as would be expected if D_x/u^*L and L/H are kept the same as in Fig. 3. Figure 7 shows horizontal patchiness as a function of the dimensionless horizontal dispersion coefficient, D_x/u^*L, for three values of F, if $L/H = 28.6$ (as in Fig. 3) and $W = 2$ m s^{-1}.

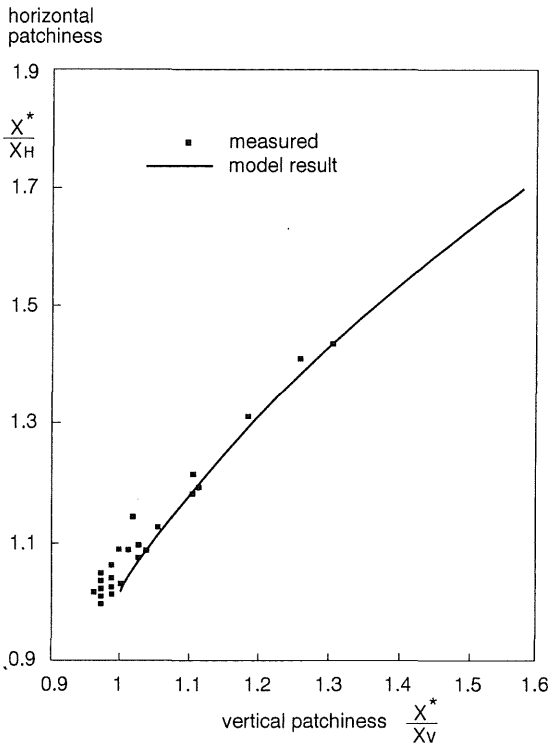

Fig. 4. Comparison between steady state model results and data from George and Edwards (1976) of the relationship between horizontal and vertical patchiness of blue-green cells in Eglwys Nynydd.

This dimensionless coefficient can be physically interpreted as the ratio between horizontal and vertical circulation or as the ratio between Livingstone-type and conveyor-belt-type circulation. If this ratio goes to 0, horizontal patchiness attains very high values, especially for higher values of F. The higher the ratio (i.e. the more important Livingstone-type circulation is compared to conveyor-belt circulation), the more homogeneous the plankton concentration.

The differences in results between my model and the model of Webster (1990) are shown in Fig. 7. Webster neglected horizontal dispersion and used the measured horizontal patchiness in Eglwys Nynydd (~ 1.25 at $W = 2$ m s^{-1}) to fit a value to F. He obtained the value $F \approx 0.9$ m d^{-1}; this parameter value is depicted in Fig. 7 at the point $X^*/\bar{X} = 1.25$, $D_x/u^*L = 0$. Note that my model produces curves that progressively approach the ordi-

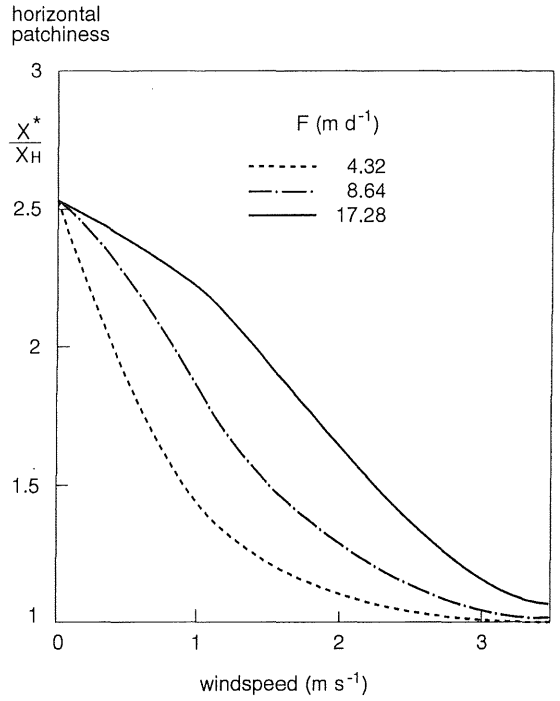

Fig. 5. Steady state model results of horizontal patchiness as a function of windspeed for three values of flotation velocity. Other parameter values as in Fig. 3.

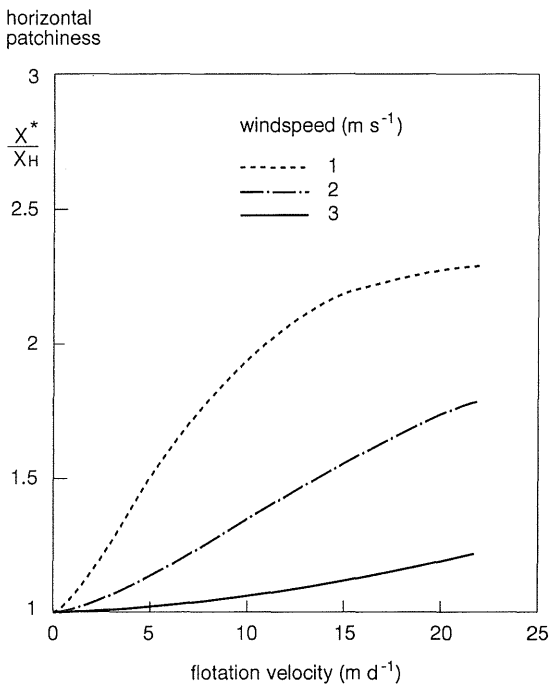

Fig. 6. Steady state model results of horizontal patchiness as a function of flotation velocity for three values of windspeed. Other parameter values as in Fig. 3.

nate for decreasing values of F. My model reproduces the same observation of George and Edwards (1976), i.e. $X^*/\bar{X} \approx 1.25$ at $W = 2$ m s^{-1} for the parameter values $F \approx 8.64$ m d^{-1} and $D_x/u^*L = 0.83$, as shown in Fig. 7. We can conclude that the horizontal patchiness measured by George and Edwards at a specific windspeed can be reproduced with my model using a value of F an order of magnitude higher than when using Webster's model.

In the approach described here, a nominated value of flotation velocity, $F = 8.64$ m d^{-1}, has been used. This value is in the middle of the large range reported by Reynolds et al. (1987) for *M. aeruginosa,* and the simulated results have been compared to the data of George and Edwards (1976). Another approach for achieving the best fit to these data could be selecting a proper F on a trial-and-error basis while keeping the other parameters fixed.

From inspection of the experimental data given in Fig. 3 and the relation between horizontal patchiness and F given in Fig. 6, it seems that if the last approach is followed, a somewhat lower best-fit value ($F \approx 8.0$ m d^{-1}) would be the result.

Extrapolation of non-steady state model results to larger lakes—Finally, we give attention to non-steady state model results. These results become more important with increases in the adjustment time, T_{max}. According to Eq. 40, T_{max} increases with the horizontal dimension of the lake and with decreasing windspeeds. Therefore, non-steady situations are important in large lakes at reasonably low windspeeds.

In this non-steady state model exercise, we consider a lake with a length in the wind direction of 10 km and a water depth (or in a stratified situation, the depth of the epilimnion) of 10 m. T_{max} for this lake at a windspeed of 3 m s^{-1} is ~10 d according to Eq. 40. (Note that for this larger lake, the prerequisite for justification of the conservative substance approach of algal cells is hardly fulfilled.)

Persistent calm weather conditions of this duration are infrequent; therefore a time-de-

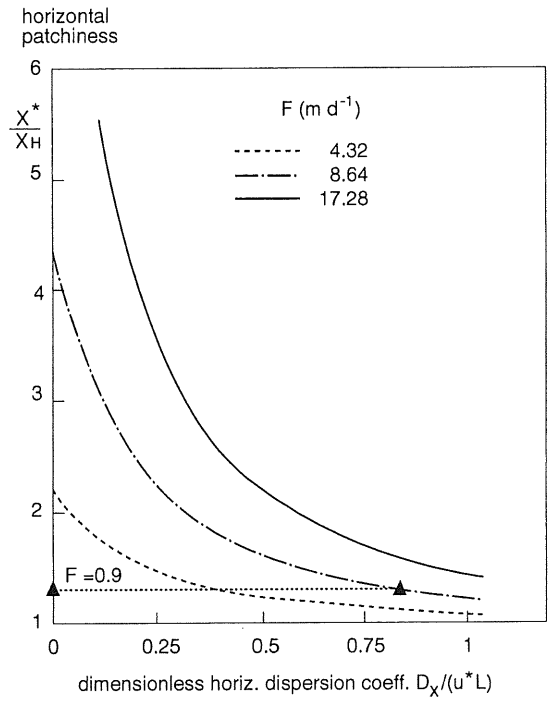

Fig. 7. Steady state model results of horizontal patchiness as a function of the dimensionless horizontal dispersion coefficient for three values of flotation velocity, keeping L/H as in Fig. 3 and $W = 2$ m s^{-1}.

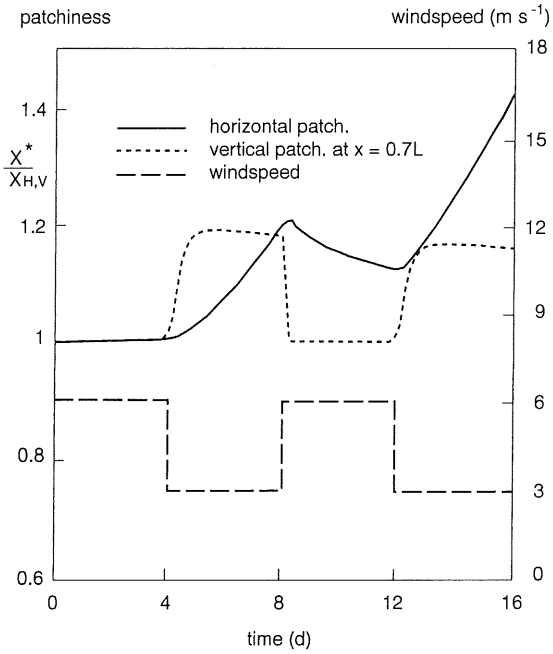

Fig. 8. Model simulation of blue-green cyanobacterial patchiness in a lake with a horizontal dimension of 10 km and a water depth or depth of epilimnion of 10 m.

pendent windspeed is introduced. A model simulation was run with wind alternating between 6 and 3 m s^{-1} every 4 d, as shown in Fig. 8. The simulated horizontal and vertical patchiness at a station located at $x = 0.7L$ is also plotted as a function of time. Starting from a homogeneous distribution of plankton, horizontal and vertical patchiness remains nearly homogeneous during the first 6 m s^{-1} windspeed period. During the next 3 m s^{-1} windspeed period, horizontal patchiness shows an exponential increase, and vertical patchiness shows a sharp increase followed by a slow decrease. In the next 6 m s^{-1} period, homogeneity is rapidly attained in the vertical direction but not in the horizontal direction. In the last 3 m s^{-1} windspeed period, vertical patchiness is comparable to the first 3 m s^{-1} period, but horizontal patchiness is substantially higher.

Figures 9 and 10 show additional results of the same simulation. Figure 9 shows the course of the plankton concentration in the surface and bottom layers at four locations during 16 d of different wind conditions. Figure 10 shows the calculated surface-layer distribution of plankton along the length of the lake at the end of the four wind periods, starting from a homogeneous distribution at $t = 0$. The figures show that an increase or a decrease in windspeed is followed by an increase or a decrease in vertical patchiness within half a day, corresponding to the fast time scale of the system: $T_{min} \approx 2H/F = 0.5 \times 10^5$s ≈ 0.5 d. It is further shown that horizontal patchiness and to a lesser extent vertical patchiness do not reach a steady state situation in any of the four wind periods, especially not in the 3 m s^{-1} case. At 3 m s^{-1}, a horizontal concentration gradient builds up rapidly at the downwind shore. This concentration gradient is slowly but not completely redistributed over the whole length of the lake during the next 6 m s^{-1} wind period, resulting in an even higher concentration gradient at the end of the last simulated 3 m s^{-1} period. The results show that in large lakes it is difficult to relate concentration gradients to wind conditions measured on the same day, as T_{max} can be 2 weeks or more.

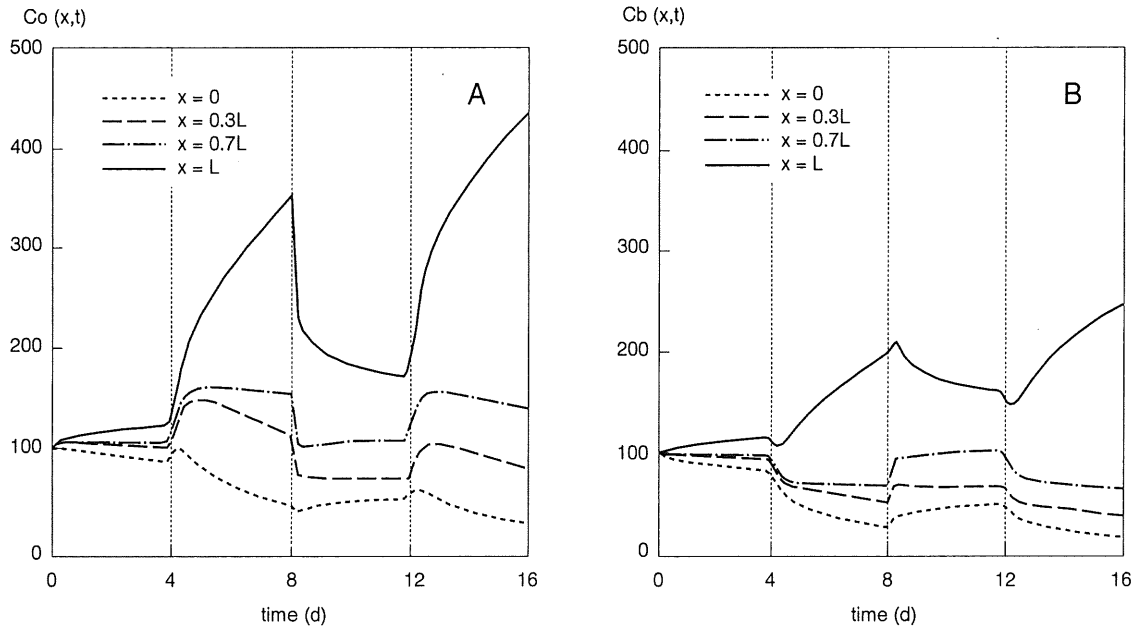

Fig. 9. A. Development of the blue-green bacterial concentration in the surface layer at four locations x measured from the upwind shore. Windspeed varies during the 16 d as in Fig. 8. B. Development of the blue-green bacterial concentration in the bottom layer at four locations with conditions as for Fig. 8.

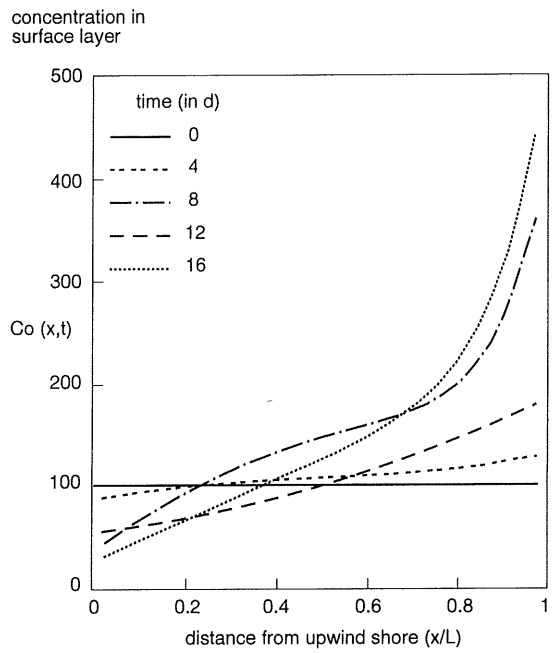

Fig. 10. Horizontal distribution of blue-green bacteria in the surface layer in the wind direction at the end of the four successive wind periods, with conditions as for Fig. 8.

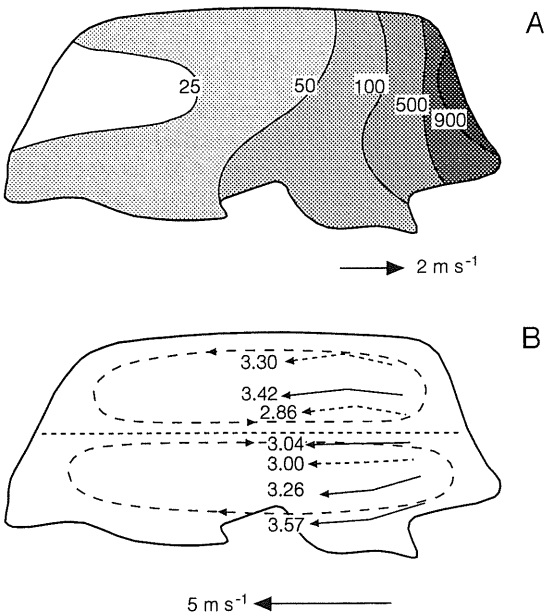

Fig. 11. A. Surface distribution of Chl *a* concentration in mg m^{-3} for a windspeed of 2 m s^{-1} in Eglwys Nynydd. B. Drogue trajectories (– – – 0.5-m and —— 1.0-m drogues) for a windspeed of 5 m s^{-1} (note that wind direction is opposite to that in panel A). (Adapted from George and Edwards 1976.)

Perspectives in future research—Remote sensing creates the potential for monitoring surface distribution patterns of blue-green cells in eutrophic lakes during clear weather conditions (Wrigley and Horne 1974). George and Edwards (1976) presented surface Chl *a* distribution patterns measured in Eglwys Nynydd. Figure 11A shows an example of such a distribution, given by them, based on 40 regularly spaced surface samples.

The concentration maximum as well as the concentration minimum are found in the wind direction along the centerline of the lake instead of near both shores parallel to the centerline. The concentration gradient in wind direction is therefore somewhat higher in the middle of the lake than along the parallel shores. However, the model predicts higher concentration gradients at lower windspeeds, hence at lower surface currents; consequently the picture of the concentration distribution leads to the impression that surface currents in the middle of the lake must be lower than near the shores parallel to the wind. This *outcome contradicts what would be expected* from Livingstone-type circulation (cf. Fig. 1). This unexpected result caused me to look more closely at the current observations made by George and Edwards. Figure 11B shows the current trajectories of 0.5- and 1.0-m free-running, depth-specific drogues measured by George and Edwards during a steady 5 m s^{-1} wind. The drift currents in the middle of the lake are indeed somewhat less than at both shores along the wind direction; thus the *horizontal circulation* pattern in Eglwys Nynydd probably *rotates in the opposite direction compared to Livingstone-type circulation.*

In a personal communication, D. G. George confirmed his observations of the existence of this reversed circulation pattern in Eglwys Nynydd. The only explanation he could offer for the measured nearshore acceleration of the wind-driven current was that any waves that break on the gently sloping concrete shoreline of the man-made reservoir tend to generate a longshore drift current.

The example above clearly shows that remote sensing of surface Chl *a* distributions could validate models of complex large-scale horizontal current patterns caused by low and medium windspeeds in a lake.

References

BANKS, R. B. 1975. Some features of wind action in shallow lakes. Proc. Am. Soc. Civ. Eng. **101:** 813–827.

CHEUNG, T. K., AND R. L. STREET. 1988. The turbulent layer in the water at an air–water interface. J. Fluid Mech. **194:** 133–151.

FISCHER, H. B., E. J. LIST, R. C. Y. KOH, J. IMBERGER, AND N. H. BROOKS. 1979. Mixing in inland and coastal waters. Academic.

GEORGE, D. G. 1981. Wind-induced water movements in the south basin of Windermere. Freshwater Biol. **11:** 37–60.

———, AND R. W. EDWARDS. 1976. The effect of wind on the distribution of chlorophyll *a* and crustacean plankton in a shallow eutrophic reservoir. J. Appl. Ecol. **13:** 667–690.

IMBERGER, J., AND J. C. PATTERSON. 1991. Physical limnology. Adv. Appl. Mech. **27:** 303–475.

KRANENBURG, C. 1987. Turbulent surface boundary-layer induced by an offshore wind. J. Hydraul. Res. **25:** 53–66.

LIVINGSTONE, D. A. 1954. On the orientation of lake basins. Am. J. Sci. **252:** 1–142.

OKUBO, A. 1971. Horizontal and vertical mixing in the sea, p. 89–168. *In* D.W. Hood [ed.], Impingement of man on the oceans. Wiley.

REYNOLDS, C. S. 1971. The ecology of the planktonic blue-green algae in the North Shropshire meres. Field Stud. **3:** 409–432.

———, R. L. OLIVER, AND A. E. WALSBY. 1987. Cyanobacterial dominance: The role of buoyancy regulation in dynamic lake environments. N. Z. J. Mar. Freshwater Res. **21:** 379–390.

SMALL, L. F. 1963. Effect of wind on the distribution of chlorophyll *a* in Clear Lake, Iowa. Limnol. Oceanogr. **8:** 426–432.

SMITH, I. R. 1979. Hydraulic conditions in isothermal lakes. Freshwater Biol. **9:** 119–145.

———. 1992. Hydroclimate: The influence of water movement on freshwater ecology. Elsevier.

WEBSTER, I. T. 1990. Effect of wind on the distribution of phytoplankton cells in lakes. Limnol. Oceanogr. **35:** 989–1001.

WRIGLEY, R. C., AND A. G. HORNE. 1974. Remote sensing and lake eutrophication. Nature **250:** 213–214.

Submitted: 3 May 1993
Accepted: 18 November 1993
Amended: 26 January 1994